Optimization of Magnetization State Manipulation in Variable-Flux PMSMs

Marcos Orviz
Dept of Elect. Computer & System Engineering
University of Oviedo
Gijón, 33204, Spain
orvizmarcos@uniovi.es

Diego F. Laborda
Dept of Elect. Computer & System Engineering
University of Oviedo
Gijón, 33204, Spain
dflaborda@uniovi.es

David Reigosa
Dept of Elect. Computer & System Engineering
University of Oviedo
Gijón, 33204, Spain
diazdavid@uniovi.es

Juan Manuel Guerrero
Dept of Elect. Computer & System Engineering
University of Oviedo
Gijón, 33204, Spain
guerrero@uniovi.es

Fernando Briz
Dept of Elect. Computer & System Engineering
University of Oviedo
Gijón, 33204, Spain
fernando@isa.uniovi.es

***Abstract*—Variable-flux permanent magnet synchronous machines (VF-PMSMs) were proposed to avoid the additional losses of conventional PMSMs during flux weakening (FW) operation at high speeds. These machines allow dynamic manipulation of the magnetization state (MS) of the permanent magnets (PMs). MS manipulation techniques have received therefore significant attention, most of these techniques being based on stator current injection in the rotor *d*-axis. However, the effect of Eddy currents induced in the PMs during MS manipulation has not been analyzed. This paper shows that PMs' Eddy currents during MS manipulation cannot be neglected. Different current waveforms (i.e., pulse, trapezoidal, S-curve and half sinusoidal signal) will be compared in terms of demagnetization/magnetization level, energy consumption and total harmonic distortion of the back electromotive force (BEMF) after MS manipulation process, to find the most advantageous one.[1]**

Keywords—Variable-flux, Eddy effects, magnetization, demagnetization.

I. Introduction

The use of permanent magnet synchronous machines (PMSMs) has considerably raised in recent years as they overcome other types of electric machines in terms of torque and power densities, controllability, and efficiency. However, when operating at high speeds, PMSMs require the injection of continuous negative current in the rotor *d*-axis to counteract the effect of the permanent magnets' (PMs) flux linkage (assumed that the PM flux is aligned with the rotor *d*-axis), matching the back-electromotive force (BEMF) with the available voltage in the DC link [1]. This technique is commonly known as flux weakening (FW) operation. To avoid the extra losses produced in FW operation, and its subsequent effects, variable flux PMSMs (VF-PMSMs) were proposed [2]-[5]. In this type of machines PMs' magnetization state (MS) can be dynamically changed depending on the machine operating condition, reducing the losses in FW operation compared with PMSMs [2].

MS control is therefore a critical issue in VF-PMSMs. MS control [6]-[12] techniques are summarized in Table I, MS manipulation being achieved by injecting a specific current profile in the stator of the machine. The current for MS control is typically injected in the *d*-axis (i_{ds}^{r}), although some proposals inject a combination of *d*- and *q*-axis current to (i) shape the PMs' magnetization pattern [10] and (ii) mitigate torque pulsations during MS manipulation [11]. Different current waveforms have been proposed, including pulse, trapezoidal or sinusoidal waveforms, a large variation of current injection time being found; the required energy for MS manipulation was only analyzed in [12] concluding that the current pulse transient duration should be minimized to reduce the injected energy.

In all methods shown in Table I, the Eddy currents induced in the PMs due to the injected current for MS manipulation were not taken into account, resulting therefore in a uniform MS independently of the current pulse waveform type and injection time, i.e., the MS depending only on the peak value of the injected current. However, Eddy currents resulting from the injected current for MS manipulation are naturally induced in the PMs. In this case, not only the current magnitude but also the waveform type and injection time determine the final MS of the machine; non-uniform magnetization of the PMs can be therefore reached in this case. The magnetization / demagnetization process in a VF-PMSM considering the effect of PMs' Eddy currents has not been previously investigated.

[1]This work was supported in part by the Research, Technological Development and Innovation Programs of the Spanish Ministry of Science and Innovation, under grant PID2019-106057RB-I00.

Table I: Comparison of MS control techniques

Method	Control variable	Waveform	Time duration	Eddy Effects
[6]	i_d	Pulse	50ms	×
[7]	i_d	Trapezoidal	50ms	×
[8]	i_d	Trapezoidal	10/34ms	×
[9]	i_d	Sinusoidal/Trapezoidal	12ms	×
[10]	i_{dq}	Pulse	40ms	×
[11]	i_{dq}	Trapezoidal	50ms	×
[12]	i_d	Pulse	12/15ms	×

This paper analyzes the effect of the injected current for MS manipulation (waveform, and injection time) on the final PMs' MS, and the required energy consumption considering PMs' Eddy current effects. Four different current waveforms will be analyzed, i.e., pulse, trapezoidal, half sinusoidal and S-curve. The required energy to reach a certain MS will be used as a metric to quantify the effectiveness of each waveform.

The paper is organized as follows: Section II analyzes the effects of Eddy currents on PMs' due to MS manipulation; Section III analyzes different current waveforms for MS manipulation; Section IV develops a comparative analysis among the different type of signals for MS manipulation. Conclusions are finally given in Section V.

Table II: Machine characteristics	
Number of slots, n_s	60
Number of poles, n_p	8
PMs material	N33SH AlNiCo9
Rated current	11 A
Rated speed	3000 rpm

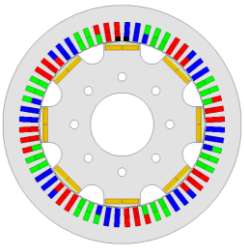

Fig. 1: Test machine 2D model.

II. Effects of Eddy Currents on PMs' MS Manipulation

In this section, the effect of Eddy currents during PMs' MS manipulation (i.e., both demagnetization and magnetization) in a VF-PMSM will be analyzed through finite element (FE) simulations. Ansys Maxwell 2D is used for this purpose. Fig. 1 shows the 2D model of the VF-PMSM test machine, its main characteristics being shown in Table II.

Fig. 2 shows the pulse current waveform that will be injected in the rotor *d*-axis to change PMs' MS, where t_{pulse} is the pulse duration and I_{peak} is the peak value of the signal.

Fig. 3 shows simulation results of PMs' MS manipulation by using a *d*-axis current pulse without considering Eddy currents in the PMs; the machine was fully magnetized before injecting the *d*-axis current pulse. Fig. 3a shows the injected

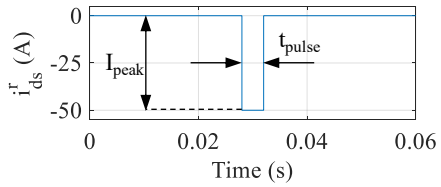

Fig. 2: D-axis pulse current waveform.

d-axis current pulse, note that the time axis has been zoomed to appreciate the pulse waveform. Fig. 3b shows the machine phase-a voltage, V_a before and after the MS manipulation process, Fig. 3c shows the required power, P, see (1), where i^r_{ds}, i^r_{qs}, v^r_{ds} and v^r_{qs} are the *dq*-axes stator currents and voltages in the rotor reference frame, respectively. Fig. 3d shows the energy consumption, E during the MS manipulation process, see (2). Fig. 3e shows the global PMs MS which is obtained from the PM flux linkage, λ_{PM} before and after the pulse current injection, which is obtained from the *d*-axis rotor flux, see (3). Finally, Fig. 3f shows the ratio between the energy consumption, E, and the level of demagnetization that the PMs have suffered due to the pulse current injection, DL (see (4), where MS_0 is the initial PMs' MS before MS manipulation and MS_f is the final PMs' MS after MS manipulation), E/DL. This ratio will be used to assess how efficient the MS manipulation process has been. Fig. 4 shows analogous results to Fig. 3 but considering the effect of Eddy currents on the PMs. It can be observed that lower P, and therefore lower energy consumption, see (2), is required to inject the current pulse (compared with the previous case, see Fig. 3). In addition, lower MS variation is achieved (for the same injected *d*-axis current as in Fig. 3). To achieve similar MS as in Fig. 3 while considering PMs' Eddy currents and keeping the same I_{peak}, t_{pulse} should be increased. Fig. 5a shows DL vs t_{pulse} both when Eddy currents on the PMs are considered and when they are not. It can be observed that, in order to obtain a similar MS considering Eddy currents than when their effect is neglected, t_{pulse} must be higher than 2ms. This occurs because increasing the pulse duration gives more time to the Eddy currents to fade away; their effect being minimized when t_{pulse}>2ms for this particular machine. Fig. 5b shows

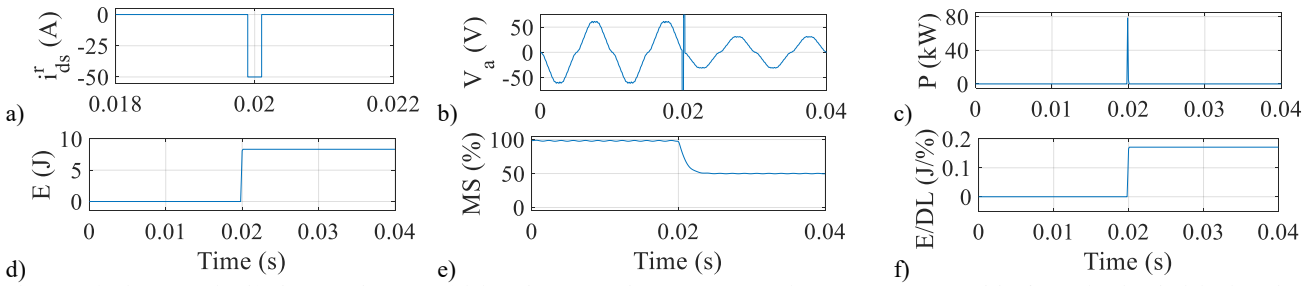

Fig. 3: a) *d*-axis current, i_{ds}^r, b) phase-a voltage, V_a, c) injected power, P, d) energy consumption, E, e) PMs' MS and f) E/DL ratio after the injection of a *d*-axis current pulse for PMs' demagnetization without considering the effects of Eddy currents on the PMs. I_{peak}=-50A, t_{pulse} = 200μs, ω_r=1500rpm, I_q=0A.

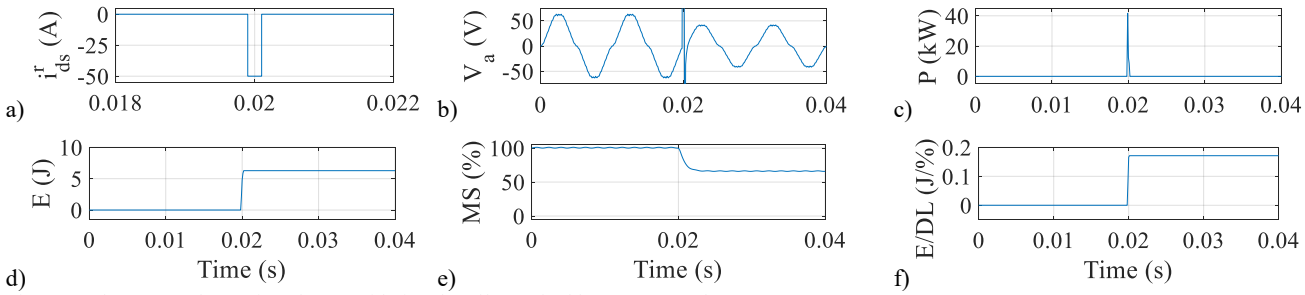

Fig. 4: Analogous results to Fig. 3 but considering the effects of Eddy currents on the PMs.

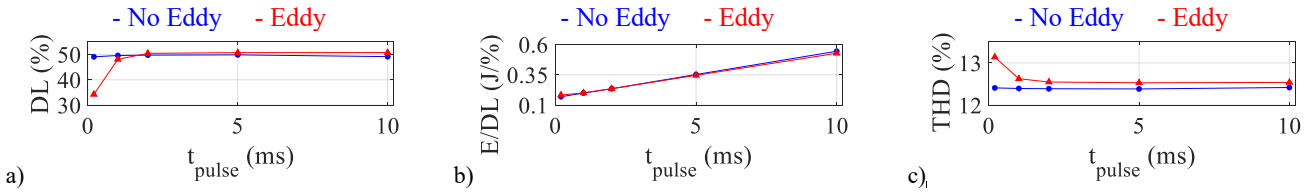

Fig. 5: a) Demagnetization level, DL, b) E/DL ratio, and c) THD of V_a after the injection of a *d*-axis current pulse for PMs' demagnetization with and without considering the effects of Eddy currents on the PMs for different t_{pulse} durations. I_{peak}=-50A, ω_r=1500rpm, I_q=0A.

E/DL vs t_{pulse}, the same tendencies are followed in both cases. This behavior is the expected one since, when Eddy currents are not considered, higher DLs can be reached (see Figs. 5a) compared to when they are taken into account, but higher E is also required (see Figs. 3 and 4d), the ratio E/DL keeping thus constant in both cases. Finally, Fig. 5c shows the THD of the BEMF vs t_{pulse}, this metric is seen to follow inverse tendency than DL, i.e., the higher the PM is demagnetized, the lower the THD will be. This can occur due to the change in the machine saturation (e.g., in the flux bridges, rotor poles, etc.); this is a subject of ongoing research.

$$P = 3/2 \cdot \left(v_{ds}^{r} \cdot i_{ds}^{r} + v_{qs}^{r} \cdot i_{qs}^{r}\right) \quad (1)$$

$$E = \int_0^t P \cdot dt \quad (2)$$

$$\lambda_{ds}^{r} = L_{ds} i_{ds}^{r} + \lambda_{PM} \quad (3)$$

$$DL = MS_0 - MS_f \quad (4)$$

$$THD = \frac{\sqrt{\Sigma_2^{\infty} V_n^2}}{V_1} \quad (5)$$

$$ML = MS_f - MS_0 \quad (6)$$

Figs. 6-8 show analogous results to Figs. 3-5 for the case of PM remagnetization, the AlNiCo PMs are fully demagnetized at the beginning of the simulation while the NdFeB PMs are fully magnetized. It can be observed that, similarly to the PMs demagnetization case, the energy required to inject the same current pulse (see Figs. 6a and 7a) is higher when Eddy currents are not considered (see Figs. 6d and 7d). Moreover, the magnetization level, ML, see (6), due to the pulse current injection is lower when the Eddy effects are considered (see Figs. 6e and 7e).

Fig. 8 shows a comparison of ML, E/ML and THD when Eddy effects are considered and when they are not. Fig. 8a shows that, when Eddy effects are considered, in order to reach a similar MS than when they are not, t_{pulse} must be higher than 2ms, i.e., the minimum pulse duration that allow Eddy currents to fade away during the magnetization process is equivalent to that one during demagnetization (see Figs. 5a and 8a). To assess the efficiency of the MS manipulation process, E/ML must be used instead of E/DL when PMs remagnetization process is analyzed. This metric is seen to be barely affected by the effects of Eddy currents (see Fig. 8b), i.e., when Eddy currents are not considered, higher ML can be reached but higher E is also required. Finally, Fig. 8c shows THD vs t_{pulse}, which is seen to follow the same tendency than ML, i.e., the higher ML, the higher the THD of the BEMF will be. It can be concluded that those conclusions reached for the demagnetization process also apply for the remagnetization one.

From the previous discussion it can be concluded that the effects of Eddy currents on PMs during the MS manipulation process must be considered since they have a significant influence in relevant aspects like the final MS of the PMs and the energy consumption during the MS manipulation process. Moreover, the duration of the demagnetization/magnetization pulse has been shown to be a key aspect for MS manipulation.

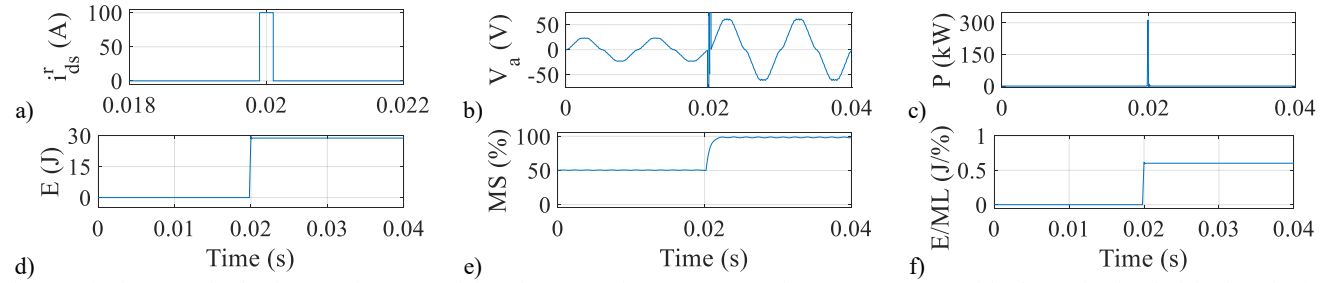

Fig. 6: a) *d*-axis current, i_{ds}^{r}, b) phase-a voltage, V_a, c) injected power, P, d) energy consumption, E, e) PMs' MS and f) E/ML ratio after the injection of a *d*-axis current pulse for PMs' magnetization without considering the effects of Eddy currents on the PMs. I_{peak}=100A, t_{pulse} = 200μs, ω_r=1500rpm, I_q=0A.

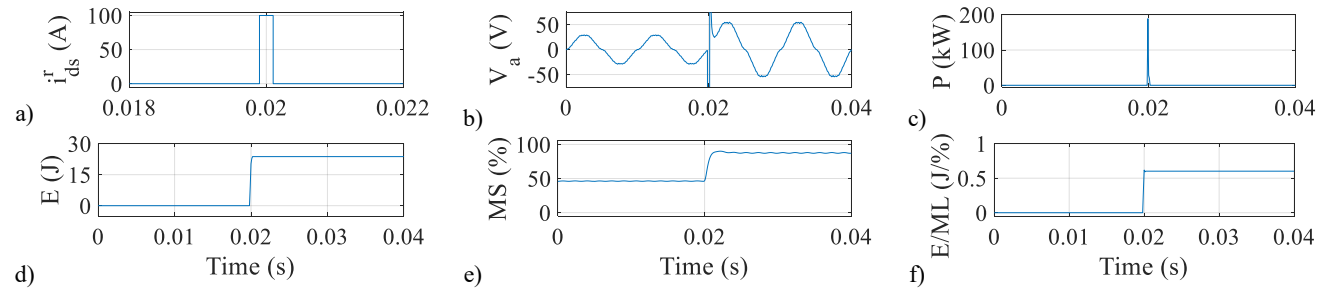

Fig. 7: Analogous results to Fig. 6 but considering the effects of Eddy currents on the PMs.

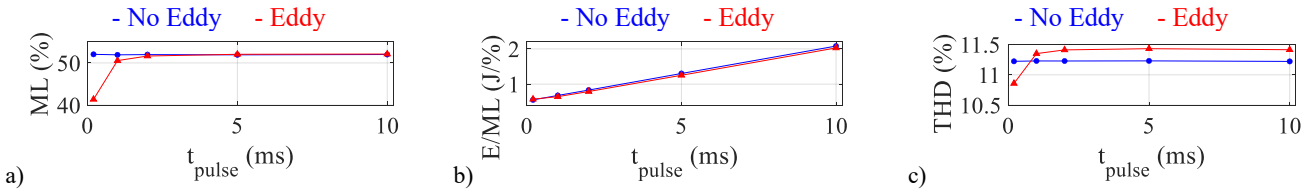

Fig. 8: a) Magnetization level, ML, b) E/ML ratio, and c) THD of V_a after the injection of a *d*-axis current pulse for PMs' magnetization with and without considering the effects of Eddy currents on the PMs for different t_{pulse} durations. I_{peak}=100A, ω_r=1500rpm, I_q=0A.

Therefore, alternative signal waveforms will be also analyzed to find the most convenient one.

III. Analysis of Alternative Signals for MS Manipulation

This section analyzes the use of three alternative waveforms for MS manipulation in VF-PMSMs considering the effects of Eddy currents on the PMs: trapezoidal, S-curve and sinusoidal.

1) Trapezoidal signal injection

Fig. 9 shows the trapezoidal current waveform that will be used for PMs demagnetization, where t_{slope} indicates the time duration of the rising/falling slope, t_{ss} indicates the constant current injection time of the trapezoidal waveform, and $t_{trap}=t_{ss}+2\cdot t_{slope}$, I_{peak} being the peak value of the signal. The same signal with opposite amplitude sign will be used for PMs remagnetization. Different combinations of t_{ss} and t_{slope} will be compared to find the most advantageous one in terms of PMs DL, E/DL, ML, E/ML and THD of V_a.

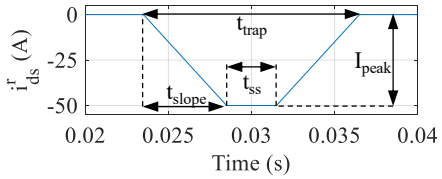

Fig. 9: D-axis trapezoidal current waveform.

Fig. 10 shows analogous results to Fig. 4 but when using a negative *d*-axis trapezoidal current injection for PM demagnetization. It can be observed that during the falling ramp of the trapezoidal waveform, P is negative (see Fig. 10c), which contributes to decrease E (see Fig. 10d) during the overall MS manipulation process.

Fig. 11a shows the PMs DL after the injection of a trapezoidal *d*-axis current signal depending on t_{slope} and for four different values of t_{ss}. It can be observed that DL increases with both t_{slope} and t_{ss}. Fig. 11b shows the ratio E/DL for the different t_{ss} and t_{slope} combinations. It can be observed that the higher t_{ss}, the higher E/DL will be, i.e., the demagnetization process will be less efficient. Therefore, it can be concluded that E/DL will be minimized for low values of t_{ss}. Moreover, an increase of t_{slope} from 0.2ms to 1ms leads to a reduction in E/DL, which can be explained by the increase of the negative P region, see Fig.10c-d. However, the longer t_{slope} is, the larger the Joule losses in the stator series resistance will be; if t_{slope} gets longer than 1ms, E/DL increases for all t_{ss} values. It can be therefore concluded that if t_{slope} is increased up to a certain value (t_{slope}=1ms for this particular machine), the active power regeneration during the falling ramp (see Fig. 10c) has higher weight than the increase of Joule losses during the MS manipulation process, the tendency reverses if t_{slope} continues getting longer. Therefore, E/DL will be minimized if $t_{slope}=t_{turn}$, where t_{turn} is the turning point in which the tendency of E/DL reverses. Finally, Fig.11c shows the THD of V_a, which, similarly to the pulse injection case (see Fig. 5c), is seen to follow an inverse tendency than DL.

Fig. 12 and 13 show analogous results to Fig. 10 and 11 but when using a positive *d*-axis trapezoidal current injection for PMs' remagnetization. It can be observed that ML and E/ML (see Fig. 13a and b) follow the same tendencies than DL and E/DL (see Fig. 11a and b), which indicates that the efficiency of the MS manipulation process will be similar regardless of whether the PMs are being magnetized or demagnetized. Therefore, the same conclusions than for the demagnetization case hold. Moreover, the THD of the BEMF is seen to follow the same tendency than ML, which matches with the results obtained for the pulse current injection (see Fig. 8c).

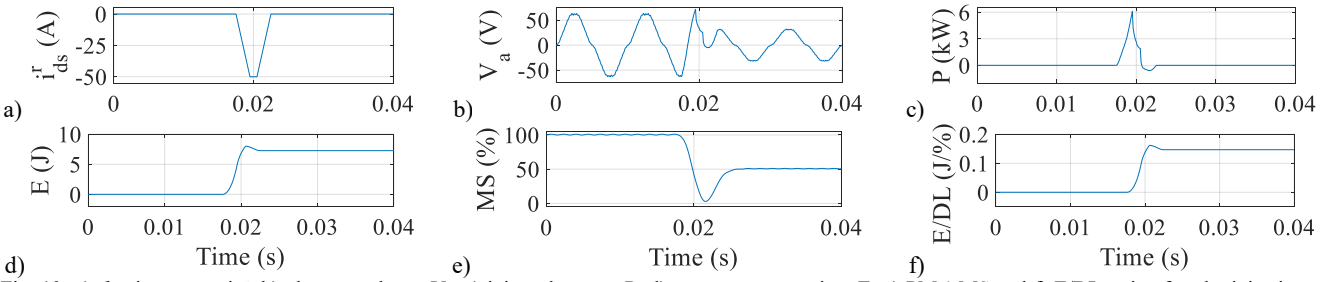

Fig. 10: a) *d*-axis current, i_{ds}^r, b) phase-a voltage, V_a, c) injected power, P, d) energy consumption, E, e) PMs' MS and f) E/DL ratio after the injection of a trapezoidal *d*-axis current for PM demagnetization. I_{peak}=-50A, t_{ss} = 1ms and t_{slope} = 2ms, ω_r=1500rpm, I_q=0A.

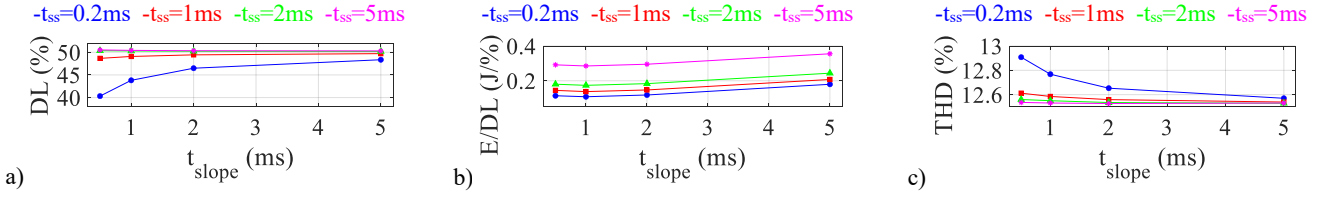

Fig. 11: a) Demagnetization level, DL, b) E/DL ratio, and c) THD of V_a after the injection of a trapezoidal *d*-axis current for PMs' demagnetization, for different combinations of t_{ss} and t_{slope}. I_{peak}=-50A, ω_r=1500rpm, I_q=0A.

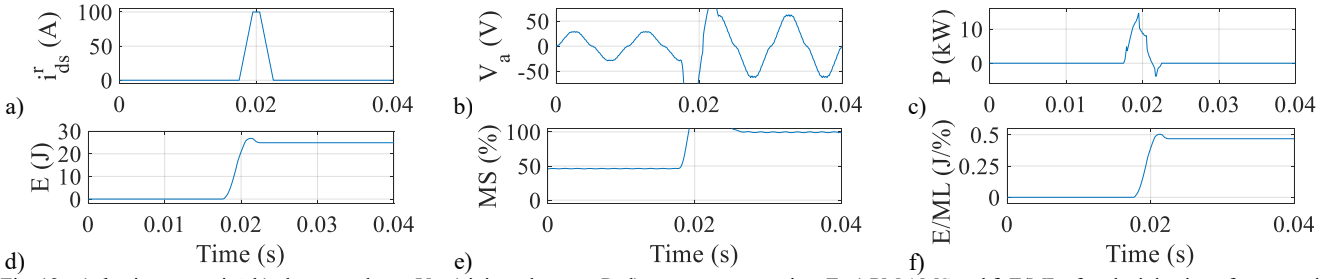

Fig. 12: a) *d*-axis current, i_{ds}^r, b) phase-a voltage, V_a, c) injected power, P, d) energy consumption, E, e) PMs' MS and f) E/ML after the injection of a trapezoidal *d*-axis current for PM magnetization. I_{peak}=100A, t_{ss} = 1ms and t_{slope} = 2ms, ω_r=1500rpm, I_q=0A.

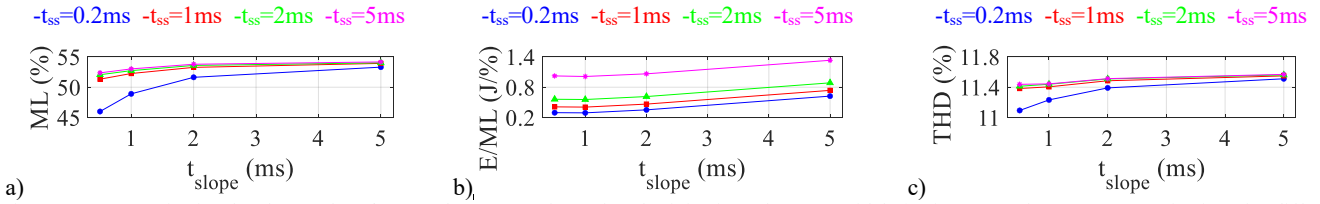

Fig. 13: a) Magnetization level, ML, b) E/ML, and c) THD of V_a after the injection of a trapezoidal *d*-axis current for PMs' magnetization, for different combinations of t_{ss} and t_{slope}. I_{peak}=100A, ω_r=1500rpm, I_q=0A.

2) Sinusoidal signal injection

Fig. 14 shows the half sinusoidal waveform that will be used for MS manipulation, where t_{sine} is the half sinusoidal signal injection time and I_{peak} is the peak value of the signal.

Fig. 15 shows analogous results to Fig. 10 but when using a *d*-axis half sinusoidal current injection. It can be observed that, similarly to the trapezoidal current case, during the falling part of the sinusoidal waveform, P is negative, also contributing to lower E during the MS manipulation process.

Fig. 16 shows analogous results to Fig. 11 but when using a *d*-axis half sinusoidal current injection. It can be observed that DL increases as t_{sine} does. Moreover, E/DL ratio decreases when t_{sine} increases up to 1ms, the tendency reverses if t_{sine} continues increasing above 1ms. Therefore, similarly to the trapezoidal waveform case, E/DL will be minimized if t_{sine}=t_{turn}=1ms for half-sinusoidal signal injection.

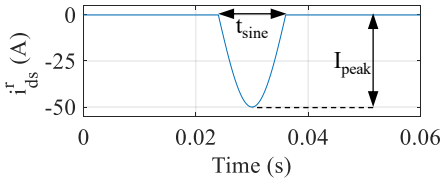

Fig. 14: D-axis half sinusoidal current waveform.

Fig. 17 and 18 show analogous results to Fig. 15 and 16 but when injecting a positive *d*-axis half sinusoidal current for PM remagnetization. Similarly to the trapezoidal current injection case, the tendencies of ML and E/ML (see Fig. 18a and b) are the same than those of DL and E/DL (see Fig. 16a and b). Therefore, the conclusions reached for the demagnetization process hold for the magnetization one.

3) S-Curve signal injection

Fig. 19a shows the S-curve waveform that will be used for MS manipulation. Equation (7) shows the mathematical expression that defines the S-curve, where t_{slope} indicates the time duration of the rising/falling slope, t_0 indicates the time instant in which half of the signal amplitude is reached during the rising ramp, and t_1 indicates the time instant in which half of the signal amplitude is reached during the falling ramp, t_{pulse} being the time difference between t_1 and t_0. One limitation of S-curves is that, if t_{slope} is too large, the signal peak value will be lower than I_{peak}; this also applies to t_{pulse}. Therefore, a trade-off between t_{pulse} and t_{slope} must be reached. This is illustrated in Figs. 19b and c. Fig. 19b represents the S-curve (see (7)) for different t_{slope} values. It can be observed that, if t_{slope}>2ms, I_{peak}=1pu is not reached. Similarly, Fig. 19c shows the S-curve (see (7)) for different t_{pulse} values, I_{peak}=1pu not being reached if t_{pulse}<5ms. Therefore, in order to reach always I_{peak}=1pu in all cases, t_{pulse}≥5ms and t_{slope} ≤2ms will be used.

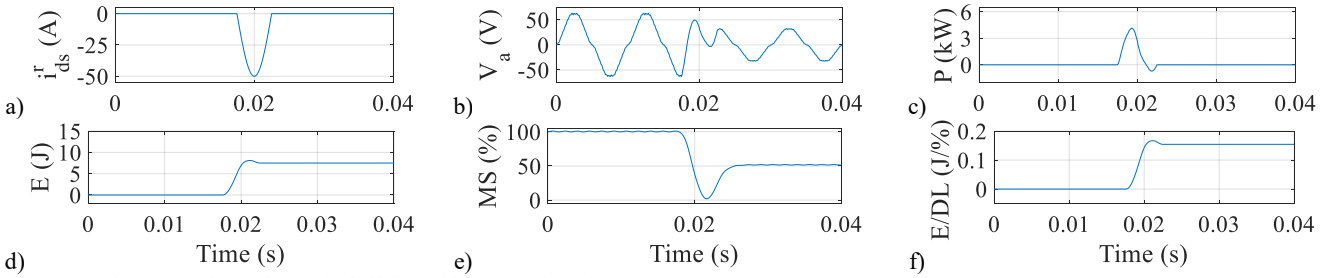

Fig. 15: Analogous results to Fig. 10 for half sinusoidal current injection, t_{sine}=5ms.

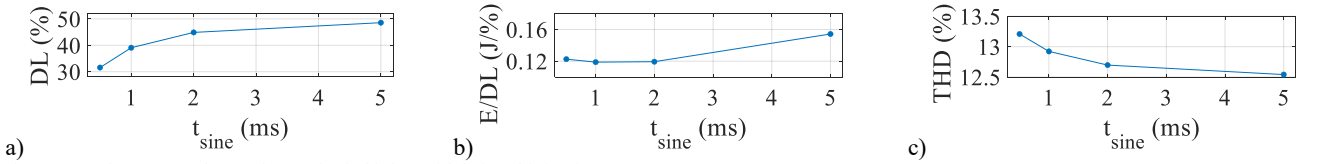

Fig. 16: Analogous results to Fig. 11 for half sinusoidal signal injection.

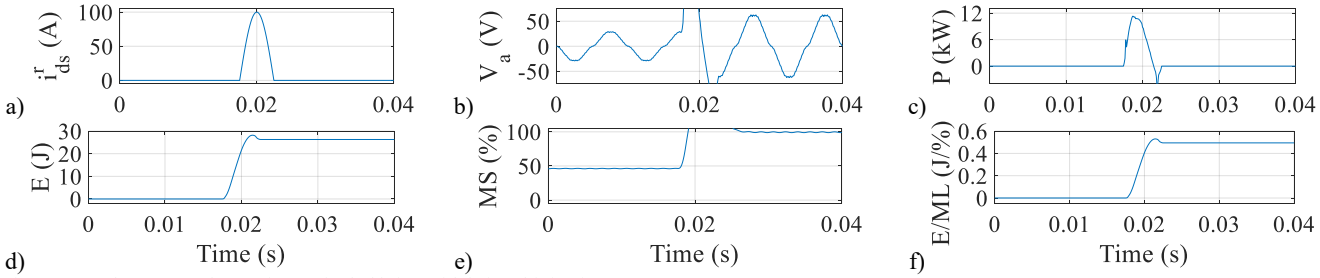

Fig. 17: Analogous results to Fig. 12 for half sinusoidal signal injection, t_{sine}=5ms.

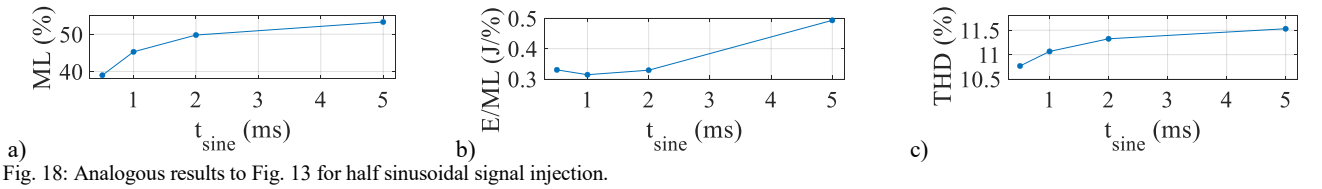

Fig. 18: Analogous results to Fig. 13 for half sinusoidal signal injection.

$$i_{ds}^{r}(t)=I_{peak}\cdot\left(\frac{1}{1+e^{-\frac{4.08}{t_{slope}}(t-t_0)}}-\frac{1}{1+e^{-\frac{4.08}{t_{slope}}(t-t_1)}}\right) \quad (7)$$

Fig. 20 shows analogous results to Fig. 15 but when using a S-curve shape current injection. Fig. 20c shows P, negative values being obtained during the falling part of the S-curve waveform, this behavior matches with that of the trapezoidal and the half sinusoidal signals.

Fig. 21 shows analogous results to Fig. 16 but when injecting an S-curve shaped current. It can be observed that E/DL ratio decreases when t_{slope} increases up to 2ms, results with longer t_{slope} are not possible to be obtained due to the inherent limitations of S-curves (see Fig. 19b). In addition, a decrease of t_{ss} from 10 to 5ms led to a reduction of E/DL, results with lower values of t_{ss} are not possible to be obtained (see Fig. 19c).

Figs. 22 and 23 show the same results as in Figs. 20 and 21 when positive *d*-axis current with S-curve shape is injected for PMs' magnetization instead of demagnetization, the same conclusions can be reached.

IV. Comparative Analysis of Signals for MS Manipulation

This section presents a comparative analysis among previously discussed waveforms, i.e., pulse, trapezoidal, half sinusoidal and S-curve.

Fig. 24 shows a) the demagnetization level, DL, b) the energy consumption, E, normalized to the DL, i.e., E/DL, and c) the THD of V_a for each waveform, depending on the total duration of each injected signal, t_{wave} (i.e., t_{pulse} for a pulse signal, t_{trap} for a trapezoidal signal, t_{sine} for a half sinusoidal signal and $t_{pulse}+2t_{slope}$ for a S-curve signal). For trapezoidal signal injection, results for t_{ss}=0.2ms and t_{ss}=1ms are only represented as both have been shown to have a superior efficiency in terms of E/DL than the remaining options (see Fig. 11b). Similarly, for S-curve current injection, results for t_{pulse}=5ms are only shown.

It can be observed that pulse current injection allows higher DLs with lower durations of t_{wave} (see Fig. 24a). However, it results in higher E/DL ratios than trapezoidal, half sinusoidal and S-curve waveforms, i.e., it requires more energy to reach a certain DL (see Fig. 24b). It is also observed that both half sinusoidal and trapezoidal (t_{ss}=0.2ms) waveforms provide the best efficiencies during the MS manipulation process in terms of E/DL ratios, the optimal results being obtained when both t_{slope} and t_{sine} = 1ms, i.e., the turning point, t_{turn}, in which the ratio of the active power regeneration over Joule losses is maximized (i.e., E/DL is minimized). Finally, Fig. 24c shows how the THD follows the inverse tendency than DL, very slight variations among the different waveforms can be observed.

Fig. 25 shows analogous results to Fig. 24 for the PMs' magnetization process, the same conclusions than for demagnetization can be reached.

From the previous discussion, it can be concluded that both half sinusoidal and trapezoidal waveforms are the most convenient options in terms of E/DL and E/ML, their performance can be optimized by finding the turning point, t_{turn} in which the ratio of the active power regeneration over Joule losses is maximized, this point will depend on the machine configuration, PM materials, temperature, etc., which is object of ongoing investigation.

V. Conclusions

This paper analyzes the effect of four current waveforms, i.e., pulse, trapezoidal, half sinusoidal and S-curve, for MS manipulation (both demagnetization and magnetization) considering PMs' Eddy current effects. It has been shown that Eddy currents in the PMs cannot be neglected during MS

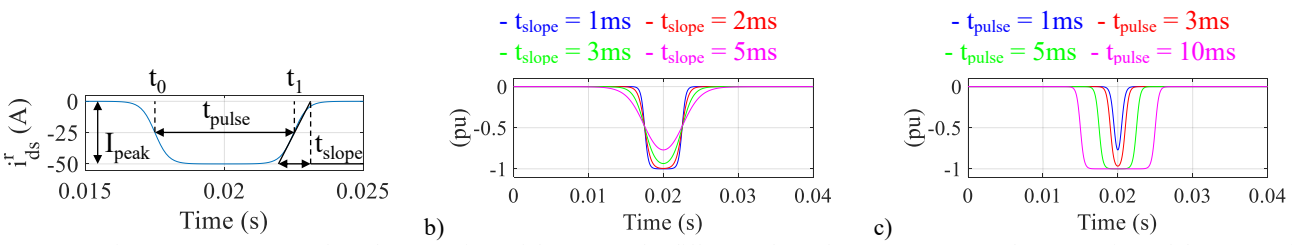

Fig. 19: a) D-axis S-curve current waveform, b) comparison of the S-curve for different values of t_{slope}, t_{pulse} = 5ms and c) comparison of the S-curve for different values of t_{pulse}, t_{slope} = 1ms, I_{peak}=1pu

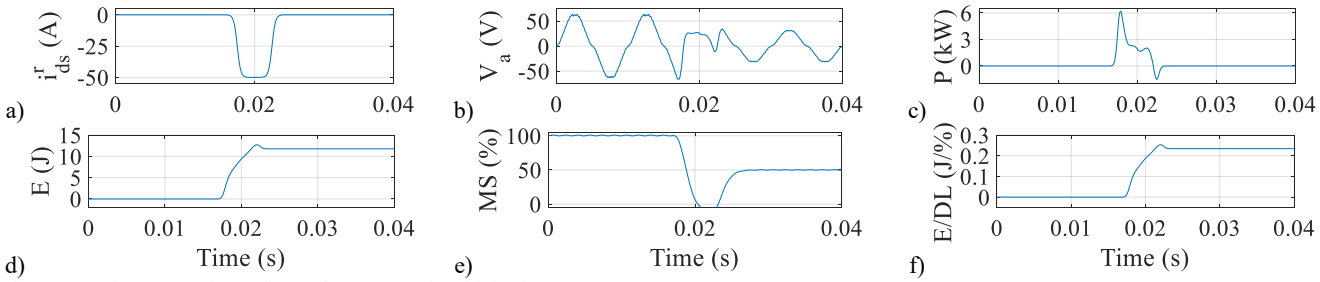

Fig. 20: Analogous results to Fig. 10 for S-curve signal injection, t_{pulse}=5ms, t_{slope}=1ms.

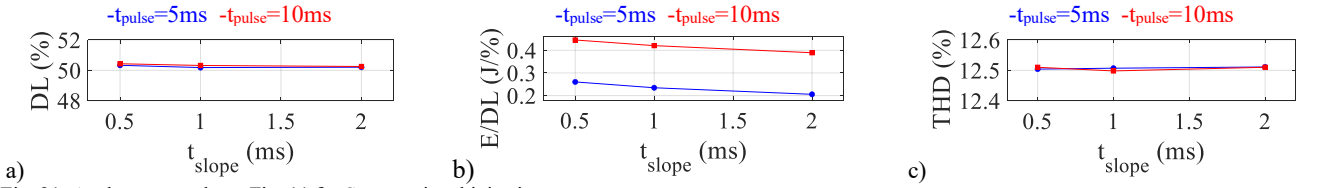

Fig. 21: Analogous results to Fig. 11 for S-curve signal injection.

manipulation. Comparison among current waveform alternatives has been made based on the required energy consumption and PMs' demagnetization/magnetization level. It has been shown that pulse current injection results in higher E/DL ratios than trapezoidal, half sinusoidal and S-curve waveforms. For trapezoidal waveform, lower ratios of E/DL were obtained when reducing t_{ss}, and increasing t_{slope} up to 1ms, the tendency reverses if t_{slope}>1ms due to the effect of Joule losses on the stator series resistance. This effect also appeared for the half sinusoidal signal as E/DL ratios were minimized if t_{sine} was increased up to 1ms. S-curves have been shown to provide worse performances than both trapezoidal and half-sinusoidal signals in terms of E/DL ratios. Neglectable variations of the harmonic distortion of the phase voltage have been found depending on the injected current waveform. Results obtained for PMs' demagnetization process have been shown to be almost equivalent for the PMs' magnetization.

REFERENCES

[1] T. M. Jahns, G. B. Kliman, and T. W. Neumann, "Interior permanent magnet synchronous motors for adjustable-speed drives," IEEE Trans. Ind. Appl., vol. IA-22, no. 4, pp. 738–747, Jul. 1986.

[2] V. Ostovic, "Memory motors," in IEEE Industry Applications Magazine, vol. 9, no. 1, pp. 52-61, Jan.-Feb. 2003, doi: 10.1109/MIA.2003.1176459.

[3] A. Athavale, K. Sasaki, B. S. Gagas, T. Kato and R. D. Lorenz, "Variable Flux Permanent Magnet Synchronous Machine (VF-PMSM) Design Methodologies to Meet Electric Vehicle Traction Requirements with Reduced Losses," in IEEE Transactions on Industry Applications, vol. 53, no. 5, pp. 4318-4326, Sept.-Oct. 2017, doi: 10.1109/TIA.2017.2701340.

[4] B. S. Gagas, K. Sasaki, A. Athavale, T. Kato and R. D. Lorenz, "Magnet Temperature Effects on the Useful Properties of Variable Flux PM Synchronous Machines and a Mitigating Method for Magnetization Changes," in IEEE Transactions on Industry Applications, vol. 53, no. 3, pp. 2189-2199, May-June 2017, doi: 10.1109/TIA.2017.2674627.

[5] M. Ibrahim, L. Masisi and P. Pillay, "Design of Variable-Flux Permanent-Magnet Machines Using Alnico Magnets," in IEEE Transactions on Industry Applications, vol. 51, no. 6, pp. 4482-4491, Nov.-Dec. 2015, doi: 10.1109/TIA.2015.2461621.

[6] T. Fukushige, N. Limsuwan, T. Kato, K. Akatsu and R. D. Lorenz, "Efficiency Contours and Loss Minimization Over a Driving Cycle of a Variable Flux-Intensifying Machine," in IEEE Transactions on Industry Applications, vol. 51, no. 4, pp. 2984-2989, July-Aug. 2015, doi: 10.1109/TIA.2015.2404918.

[7] J. Chen, J. Li and R. Qu, "Maximum-Torque-per-Ampere and Magnetization-State Control of a Variable-Flux Permanent Magnet Machine," in IEEE Transactions on Industrial Electronics, vol. 65, no. 2, pp. 1158-1169, Feb. 2018, doi: 10.1109/TIE.2017.2733494.

[8] J. Chen, J. Li and R. Qu, "Analysis, Modeling, and Current Trajectory Control of Magnetization State Manipulation in Variable-Flux Permanent Magnet Machines," in IEEE Transactions on Industrial Electronics, vol. 66, no. 7, pp. 5133-5143, July 2019, doi: 10.1109/TIE.2018.2868306.

[9] B. S. Gagas, K. Sasaki, T. Fukushige, A. Athavale, T. Kato and R. D. Lorenz, "Analysis of Magnetizing Trajectories for Variable Flux PM

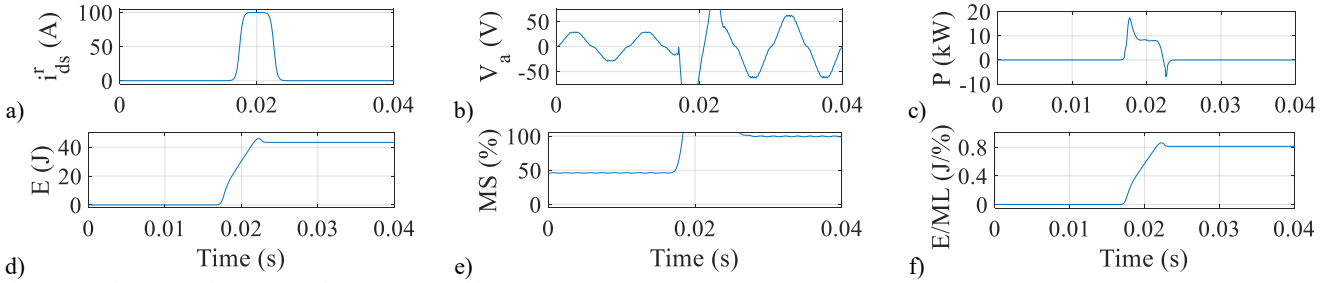

Fig. 22: Analogous results to Fig. 12 for S-curve signal injection, t_{pulse}=5ms, t_{slope}=1ms.

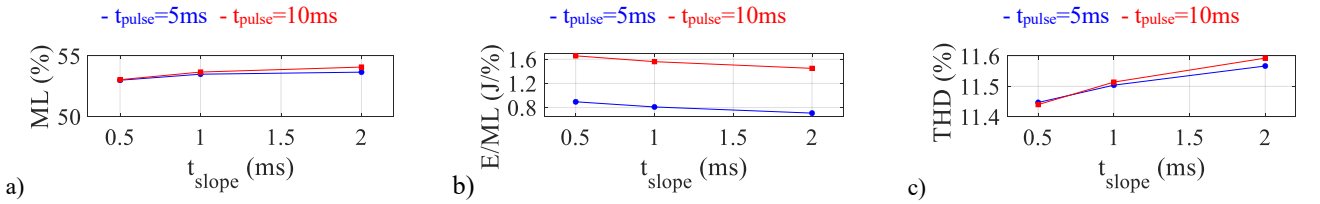

Fig. 23: Analogous results to Fig. 13 for S-curve signal injection.

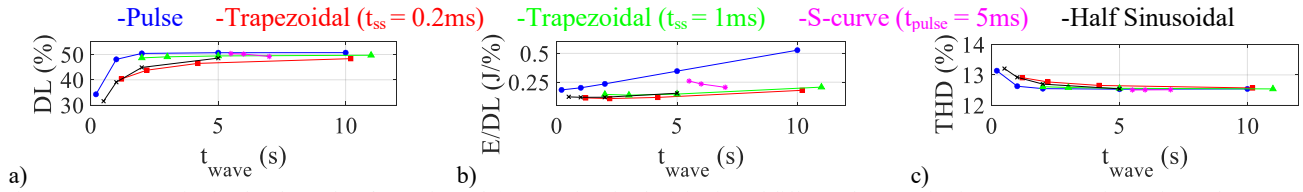

Fig. 24: a) Demagnetization level, DL, b) E/DL ratio, and c) THD of V_a for the injection of different demagnetization current waveforms (i.e., pulse, trapezoidal, half sinusoidal and S-curve) depending on the waveform duration. I_{peak}=-50A, ω_r=1500rpm, I_q=0A.

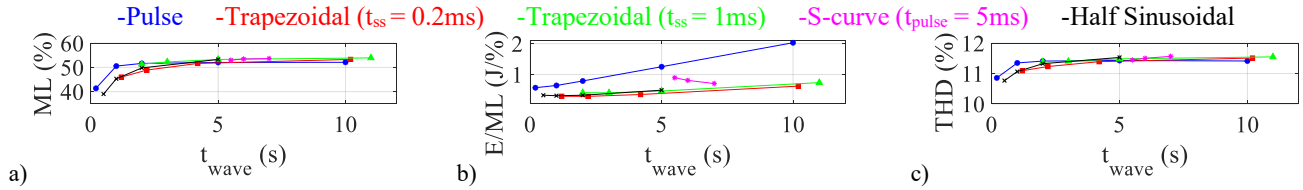

Fig. 25: a) Magnetization level, ML, b) E/ML ratio, and c) THD of V_a for the injection of different magnetization current waveforms (i.e., pulse, trapezoidal, half sinusoidal and S-curve) depending on the waveform duration. I_{peak}=100A, ω_r=1500rpm, I_q=0A.

Synchronous Machines Considering Voltage, High-Speed Capability, Torque Ripple, and Time Duration," in IEEE Transactions on Industry Applications, vol. 52, no. 5, pp. 4029-4038, Sept.-Oct. 2016, doi: 10.1109/TIA.2016.2582119.

[10] R. Imamura, T. Wu and R. D. Lorenz, "Design of Variable Magnetization Pattern Machines for Dynamic Changes in the Back EMF Waveform," in IEEE Transactions on Industry Applications, vol. 55, no. 4, pp. 3469-3478, July-Aug. 2019, doi: 10.1109/TIA.2019.2903028.

[11] C. Yu, T. Fukushige, N. Limsuwan, T. Kato, D. D. Reigosa and R. D. Lorenz, "Variable-Flux Machine Torque Estimation and Pulsating Torque Mitigation During Magnetization State Manipulation," in IEEE Transactions on Industry Applications, vol. 50, no. 5, pp. 3414-3422, Sept.-Oct. 2014, doi: 10.1109/TIA.2014.2305768.

[12] A. Takbash and P. Pillay, "Magnetization and Demagnetization Energy Estimation and Torque Characterization of a Variable-Flux Machine," in IEEE Transactions on Energy Conversion, vol. 33, no. 4, pp. 1837-1845, Dec. 2018, doi: 10.1109/TEC.2018.2837893.